Fundamentals and applications of a plasma-processing system based on electron-beam ionization[a)]

D. Leonhardt,[b)] S. G. Walton, and R. F. Fernsler
Plasma Physics Division, Naval Research Laboratory, Washington, D.C. 20375-5346

(Received 3 November 2006; accepted 1 February 2007; published online 25 April 2007)

Plasmas generated from moderate energy (2–5 keV) electron beams (e-beam) have unique, attractive characteristics that are ideal for materials processing applications. These plasmas possess low electron temperatures (<0.5 eV), variable plasma densities (10^9–10^{12} cm^{-3}) with an improved control of plasma species generation, and perhaps most importantly, a direct scalability to processing areas exceeding one square meter. These characteristics are due to the plasma ionization being driven by the e-beam instead of an external electromagnetic field as used in conventional processing plasma sources. Theoretical and experimental system details are discussed in terms of plasma operating conditions applied to three different surface modification approaches: metal nitriding, negative ion etching, and polymer surface energy tailoring. [DOI: 10.1063/1.2712424]

I. INTRODUCTION

Although the possible use of electron beams to generate plasmas had been discussed[1] in the early 1980s, the paradigm of a scalable large area electron beam generated plasma had been addressed first by Fernsler *et al.*[2] Subsequent work addressed theoretical refinements[3] as well as early experimental studies[4–6] of these plasmas generated by 2–5 keV electron beams. In the past few years, the attributes afforded by these systems have been exploited, illustrating their flexibility and reliability. Applications to etching,[7,8] surface hardening,[9,10] and thin film deposition[11,12] have all been discussed, as well as new outgrowths into polymer modification[13,14] in general review articles.

In this work, a general overview of electron beam (e-beam) generated plasmas is given with substantial experimental support from *in situ* diagnostics (Langmuir probe and ion mass spectrometry) for electron-ion and ion-ion plasmas. The variation in surface ion fluxes is discussed in detail, with respect to the bulk plasma properties and surface biasing conditions. In the final section we describe recent advances using these plasmas to nitride titanium surfaces and to tailor the surface free energy of polyethylene and polyimide materials.

II. OVERVIEW OF E-BEAM GENERATED PLASMAS

A. E-beam ionization and plasma formation

Since e-beam generated plasmas do not use an electromagnetic (EM) field to heat the plasma electrons, they are colder than in conventional plasma processing sources, the gas remains near room temperature and plasma generation is unusually efficient. To understand these claims better, consider the electron collision cross sections for nitrogen shown in Fig. 1(a). A typical Maxwellian electron energy distribution (EED) with a temperature T_e=4 eV has also been superimposed on the semilog plot. This EED is representative of a general plasma discharge created and sustained by an EM field heating the free electrons. As can be seen by this representation, only a small portion of the high energy tail of the EED contributes to ionization[15] in discharges, while the bulk of the plasma electrons merely excite the gas. Therefore, the energy being supplied to sustain the discharge is primarily going into inelastic collision processes (excitations), which ultimately heat the plasma gas. The plasma gas temperature is typically equal to the plasma ion temperature ($T_{gas} \cong T_{ion}$), and as the ion temperature increases the ion anisotropy at the substrate decreases. Hence, the inefficient use of applied power leads to gas heating that can produce a detrimental effect on the ion anisotropy.

When a 2 keV electron passes through a gas [Fig. 1(b)] the dominant cross section is ionization, therefore ionization is directly tied to the e-beam current and efficient. The second largest cross section is usually dissociation (dashed line) in molecular gases, and therefore e-beams produce large populations of radicals as well. Secondary (i.e., plasma) electrons can be created over the entire e-beam energy range, although most are born with low energies. Moreover, since there are no applied EM fields to heat the electrons, they lose energy through collisions with the gas molecules. Thus, the plasma EED is limited to the lowest threshold process of the gas, typically a ground state vibrational excitation of energy ~0.5 eV. However, from Fig. 1 it can be seen that the electron-molecule collision cross section depends strongly on the electron energy and therefore the inelastic cooling of the electrons is not constant. For example, in 50 mTorr of nitrogen, the plasma electrons take roughly 2 μs to cool to 1 eV, and roughly 70 μs to cool below 0.5 eV.

B. E-beam propagation

The interaction of e-beams with the background gas and plasma has been discussed in detail previously[2,3] and here only a brief synopsis of the beam scattering and instabilities is included. Inelastic scattering (ionization, dissociation)

[a)]Paper CI2 3, Bull. Am. Phys. Soc. **51**, 59 (2006).
[b)]Invited speaker. Present address: Fusion UV Systems, Inc., Gaithersburg, MD. Electronic mail: dleonhardt@fusionuv.com

Downloaded 26 Apr 2007 to 132.250.158.37. Redistribution subject to AIP license or copyright, see http://pop.aip.org/pop/copyright.jsp

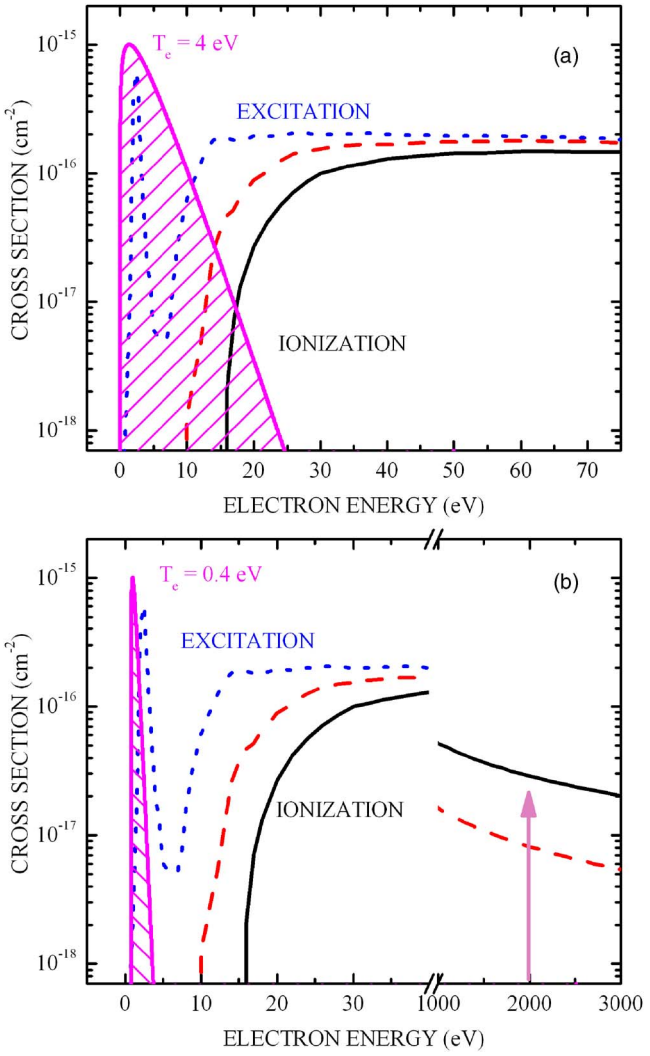

FIG. 1. (Color online) Electron impact excitation (dotted), dissociation (dashed), and ionization (solid) cross sections for nitrogen. (a) A conventional plasma electron energy distribution with T_e=4 eV is superimposed. (b) A 2 keV electron beam and resultant plasma T_e=0.4 eV electron energy distribution are superimposed.

causes the beam energy to decrease as it propagates through the background gas. The energy lost by the e-beam as the beam passes through the background gas is given by the classical expression $d\varepsilon_b/dz \propto [ZN \ln(\varepsilon_b)]/\varepsilon_b$ where ε_b is a scaled beam energy, z is the propagation distance, Z and N are the atomic number and gas density, respectively. Thus, high gas densities N require high beam energy ε_b to maintain the same beam propagation distance. For common gases (Ar, N_2, O_2), a 2 keV beam will lose approximately 15% of its energy after traveling 1 m in 50 mTorr. However, the electron beam will also scatter elastically off the gas molecules. These collisions cause the beam to spread laterally at a rate given by $d(\cos\theta)/dz = N\sigma_m$, where θ characterizes the angular beam divergence and σ_m is the momentum transfer cross section produced by multiple small angle collisions. To minimize beam spreading, a longitudinal magnetic field B can be applied parallel to the beam axis. In this case, the beam radius r_b grows as $d(r_b^2)/dz \cong 4N\sigma_m(v_b/\omega_c)^2$, where v_b is the beam velocity, $\omega_c = eB/mc$ is the electron cyclotron frequency, e is the electron charge, m is the electron mass, and c is speed of light. In practice, a magnetic field of 100–200 Gauss is sufficient to maintain $r_b \cong 1$ cm for a 2 keV beam over a distance of 1 m.

The beam can interact with the plasma electromagnetically, by coupling energy to the plasma electrons through the two-stream instability. However, from the above discussion, collisions with the background gas cause the beam energy and velocity to spread and the instability is strongly damped once the beam velocity spread Δv_b satisfies $\Delta v_b/v_b \geq [\pi\omega_b^2/\omega_{pe}\nu_{pe}]^{1/2}$. Here, ν_{pe} is the plasma electron collision frequency and ω_b and ω_{pe} are the beam and plasma electron frequency, respectively. Over a wide operating regime of pressure, density, and energy, beam disruption has not been observed, which suggests the e-beams are created or acquire a velocity spread $\geq$20%.

III. PLASMA PARAMETERS AND PROPERTIES

The construction of pulsed systems used in our laboratories has been discussed in detail in Ref. 16 and will not be repeated here. Beams used in test systems are actually electron sheets, typically 1 cm thick and 30 cm wide with a propagation distance determined by chamber dimensions (40–100 cm). The beam energy is set at 2 keV with pulse durations of 0.1–10 ms and duty factors up to 70%. Temporally resolved plasma diagnostics for an argon plasma (50 mTorr, 6 ms pulse width, 20% duty factor) from Ref. 17 are shown in Figs. 2 and 3. The plasma parameters from Langmuir probe measurements show a low-valued, well behaved plasma potential V_{plasma} and temperature T_e during the pulse, after a brief ignition phase. The plasma density n_e continued to increase but did not saturate by the end of the e-beam pulse. The evolution of the argon ions' energy distribution is shown in Fig. 3. Near pulse end (gate A), the ion energy distribution was narrow and had a most probable energy of 2.75 eV with a slight low-energy tail due to collisions within the sheath adjacent to the electrode. When the ion energy distribution was collected nearly continuously (gate B), it broadened significantly and acquired a high energy tail as well as an additional secondary peak below 1 eV. Analysis of the time-resolved ion flux showed (see Ref. 17) that high energy ($\geq$4 eV) ions arrive in a burst during the ignition phase, while most of the lowest energy ($\leq$2 eV) ions arrived after the e-beam pulse, during the afterglow. In the afterglow, the plasma temperature dropped immediately as high energy electrons left the system. Subsequently, the plasma potential and ion energies decreased rapidly. With only low energy electrons left, the diffusion of plasma ions slowed dramatically as the ambipolar diffusion D_a coefficient decreased and the afterglow plasma persists for many milliseconds. A further complication in argon is a pronounced Ramsauer minimum in the electron-neutral cross section below 1 eV. That minimum increases the dependence of D_a on T_e in magnetized plasmas, and diffusion slows even more as T_e falls.

In a 50 mTorr nitrogen plasma (3 ms pulse, 10%–20% duty factor), the plasma equilibrated rapidly, but all are smaller than in argon. The electron density equilibrates rap-

Downloaded 26 Apr 2007 to 132.250.158.37. Redistribution subject to AIP license or copyright, see http://pop.aip.org/pop/copyright.jsp

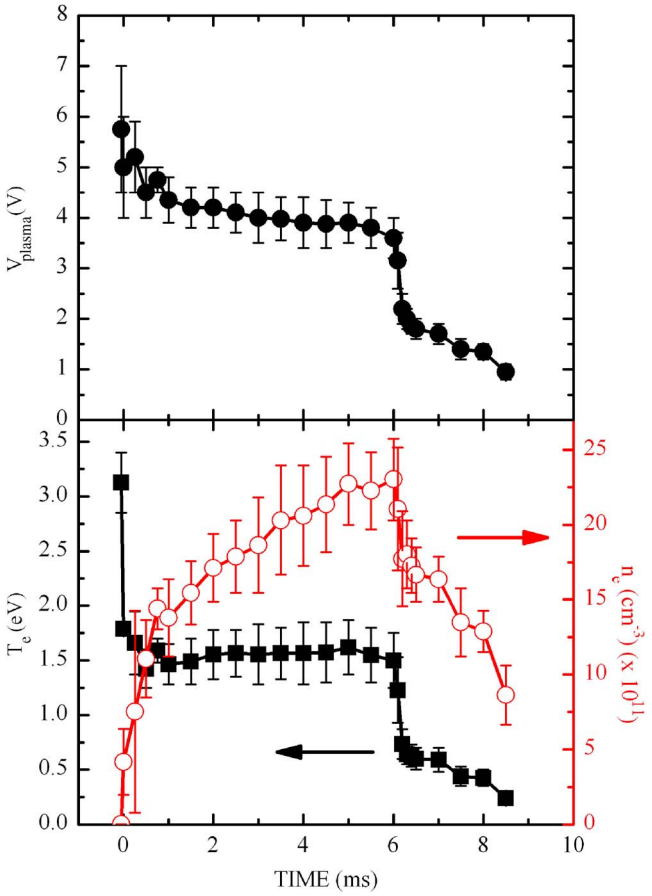

FIG. 2. (Color online) Langmuir probe data for e-beam generated plasma produced in argon. A 6 ms pulse length was used.

idly after ignition (Fig. 4, bottom), because electrons recombine quickly with molecular ions ($N_2^+ + e \rightarrow 2N$; $k_{recomb} \sim 10^{-7}$ cm^3/s). Since recombination, rather than diffusion, is the main loss mechanism for the dominant molecular ions, the plasma rapidly reaches a steady state where the production (beam ionization) and loss (recombination) processes balance. The difference between the rapid recombination loss of the molecular ions and slower decay exhibited by N^+ atomic ions can be seen in the ion flux measurements in the middle and top of Fig. 4, respectively. These two loss mechanisms account for the rapid but finite decay when the e-beam is turned off and the multiple-millisecond decay of n_e shown in the Langmuir probe measurement. In both cases, the high energy ($\geq$1.5 eV) ion fluxes are present throughout the e-beam pulse then decay quickly in the afterglow, with only a slight "peak" during ignition. The low energy molecular ions are consumed by the dissociative recombination mechanism [$dn(N_2^+)/dt \sim -\beta T_e^{-0.39}$, where β is a constant] more slowly in the afterglow while the atomic ions diffuse long into the afterglow as in the argon case.

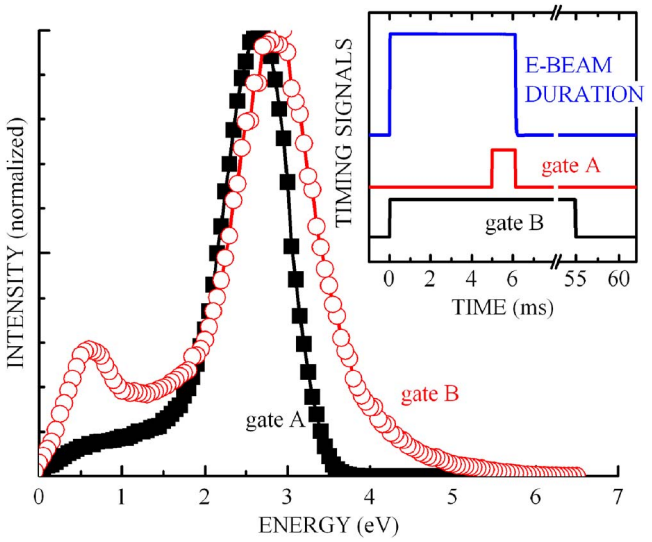

FIG. 3. (Color online) Ar^+ energy distributions for e-beam generated plasma produced in argon at an electrode 2.5 cm from the beam edge. Respective times of ion collection are shown in the inset (Gate A/B).

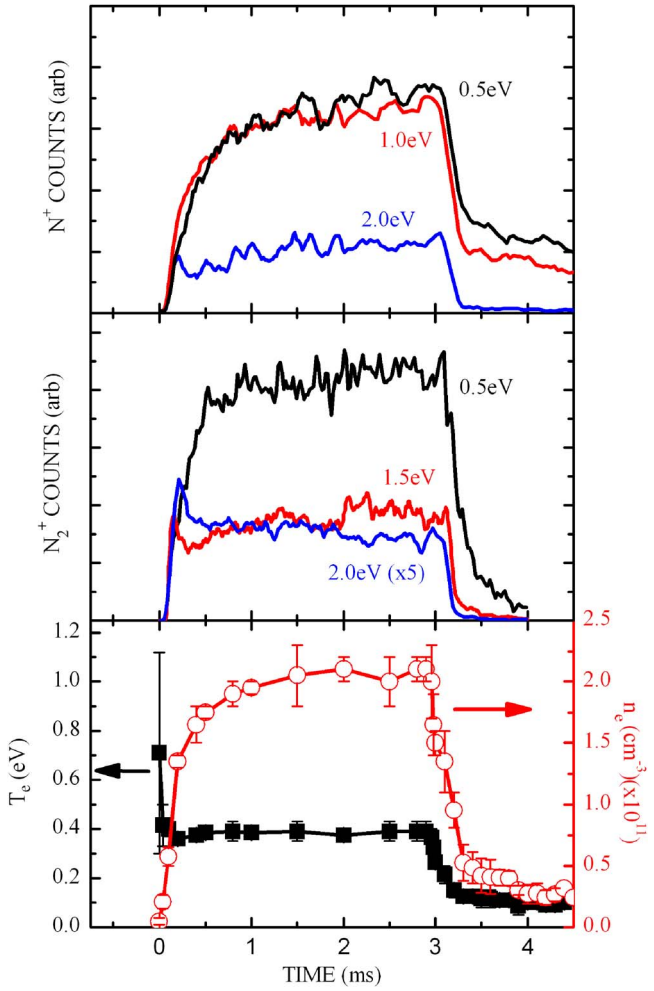

FIG. 4. (Color online) Nitrogen ion energy flux and Langmuir probe data for e-beam generated plasmas produced in nitrogen. A 3 ms pulse length was used.

IV. APPLICATIONS

Aside from scalability and high ionization efficiency, an important attribute of e-beam generated plasmas is the ability to produce dense plasmas with low electron temperatures. In this section, advantages of these capabilities are discussed. Due to the low electron temperature, e-beam generated plas-

Downloaded 26 Apr 2007 to 132.250.158.37. Redistribution subject to AIP license or copyright, see http://pop.aip.org/pop/copyright.jsp

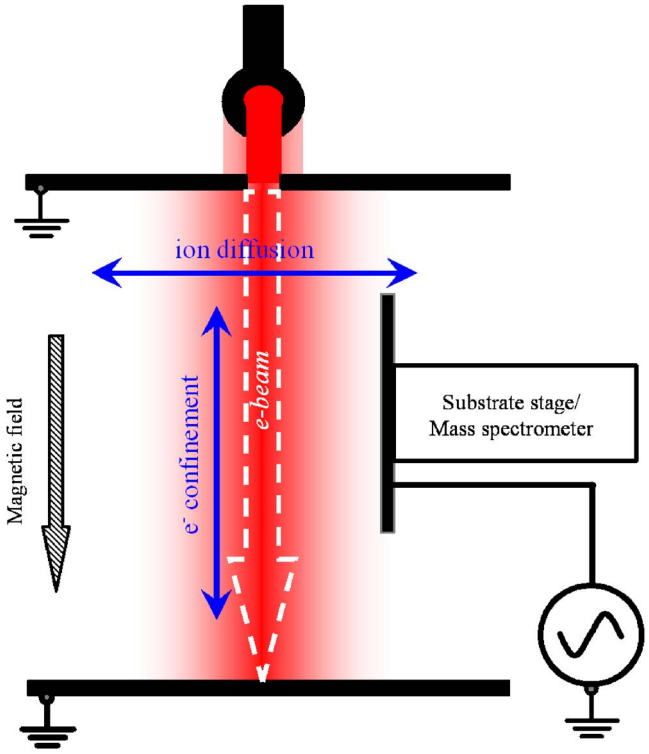

FIG. 5. (Color online) Schematic of e-beam generated system with currents labeled.

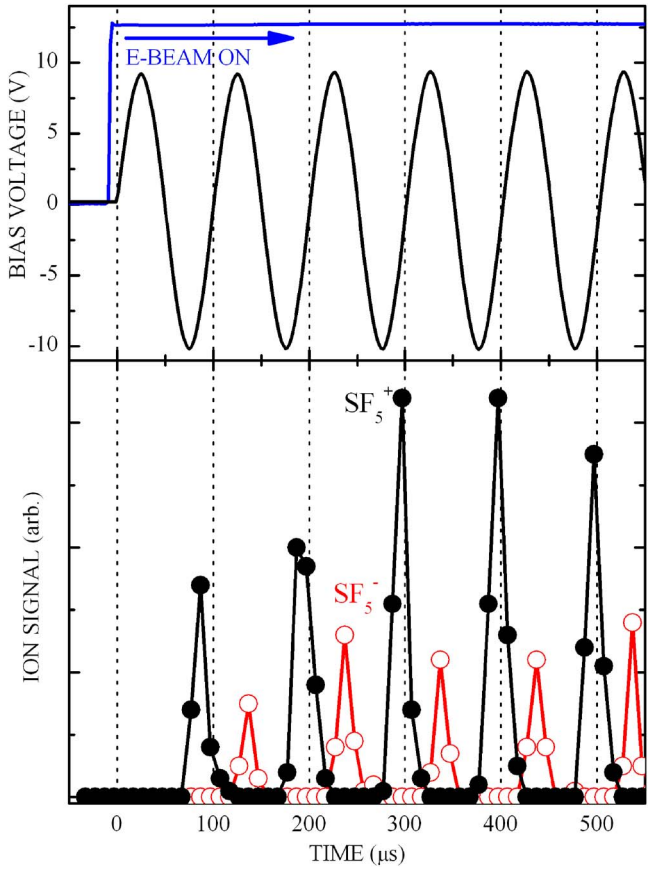

FIG. 6. (Color online) SF_5 ion flux extracted from ion-ion plasma created in 50% Ar/50% SF_6. Sinusoidal extraction voltage is shown with the plasma pulse.

mas can readily form ion-ion plasmas, where the primary negative charge carriers are ions instead of electrons. Negative ions are formed by electron attachment to electronegative gases, and in halogen-based gases such as SF_6, Cl_2, and F_2 the attachment rate is large only when electron temperature is quite low. Such plasmas are of great interest to the semiconductor manufacturing industry to reduce surface charging due to the highly mobile plasma electrons in a gate oxide etch process. Thus, similar fluxes of positive and negative ions are necessary, requiring that the production and diffusion rates of both species are comparable.

In conventional discharges, T_e is typically too large (3–4 eV) for ion-ion plasmas to form other than in the afterglow. Consequently, while most processing plasmas contain negative ions, they are almost always trapped electrostatically by the plasma potential established by the electrons. Ion-ion plasmas therefore exist only briefly in the afterglow, when T_e as well as the ion density are both small. However, the low electron temperature in e-beam generated plasmas allows a rapid and continuous conversion of electrons to negative ions. Furthermore, the magnetic field that collimates the e-beam also confines the plasma electrons, thus increasing the probability of attachment while the massive ions, which are less impacted by the magnetic field can easily cross the field lines to the substrate (see Fig. 5). To extract both polarities of ions a 10 kHz, 20 V peak-to-peak signal was applied to the mass spectrometer stage[18] in a 50% Ar/50% SF_6 plasma. The flux of each SF_5 ion at the stage is shown in Fig. 6. The ion flux closely followed the stage bias polarity implying only few plasma electrons were present. Of course, the ion currents comprised of multiple ion species: SF_6^- (65%), SF_5^- (15%), F^- (15%), and SF_5^+ (70%), Ar^+ (13%), SF_3^+ (10%), with relative fluxes is given in parentheses. The total ion currents are shown in Fig. 7, extracted with a 20 kHz, 100 V peak-to-peak signal during the last 2 ms of the e-beam pulse. The stage currents in the lower trace of Fig. 7 demonstrated a pure ion-ion plasma character as the total positive and negative ion current swings were equal. Additional biasing schemes to take full advantage of the system symmetry and the more complicated sheath effects[19] are presently being investigated.

Another attribute of e-beam generated plasmas is the production of a large concentration of atomic ions in addition to molecular ions. This attribute is advantageous for processes such as nitriding metals[9,10] where an improved control over the ion flux can greatly enhance the surface modification. Nitriding metals is important industrially because metals are selected for their intrinsic bulk properties, however it is frequently desirable to nitride the surface in order to have a harder, low-wear surface to prolong the piece lifetime. While heating the metal greatly increases the surface nitriding rate, problems arise when the surface temperature of the metal exceeds a critical phase transition temperature.

By using an e-beam generated plasma, the workpiece is greatly decoupled from the plasma production and the high flux of energetic atomic nitrogen ions[20] can more effectively penetrate the material and promote surface diffusion of atomic nitrogen species. More specifically, the large flux of

Downloaded 26 Apr 2007 to 132.250.158.37. Redistribution subject to AIP license or copyright, see http://pop.aip.org/pop/copyright.jsp

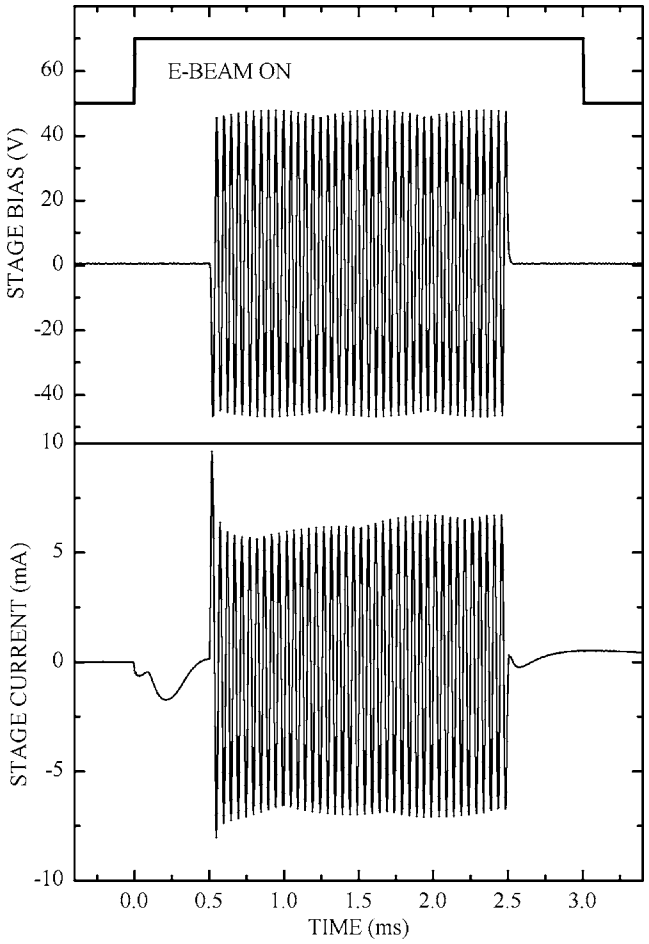

FIG. 7. Total currents extracted from Ar/SF_6 ion-ion plasma with a 20 kHz, 100 V peak-to-peak extraction signal.

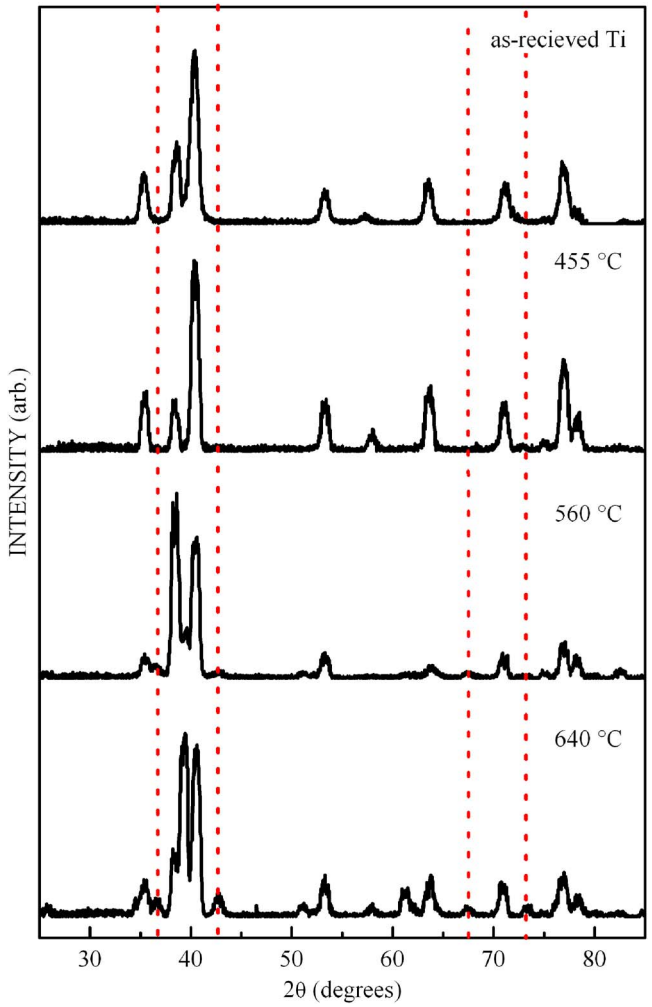

FIG. 8. (Color online) X-ray diffraction spectra of titanium nitrided in a continuous plasma source at various temperatures.

the atomic N^+ arrive at the workpiece with energies comparable to the full sheath voltage. This is due to the different ion-neutral collision mechanisms for each ion species. Atomic ions only lose energy through momentum transfer collisions while molecular ions undergo charge exchange collisions with cross sections[21] $\sigma=2.9\times10^{-16}$ and 3.1×10^{-15} cm^2, respectively. In a standard operating pressure of 120 mTorr, the mean free path $\lambda(=\sigma n_{gas})$ for the atomic ions is approximately 1 cm, whereas the mean free path for the molecular ions is approximately 0.05 cm. To go from the plasma to the surface, the ions must traverse the sheath of thickness s estimated[22] by 740 $(V_s/n_s)^{1/2}$ where V_s is the voltage applied to the workpiece in volts and n_e is the ion density at the sheath edge in cm^{-3}. In most experiments, $V_s \approx 100$ V and $n_s \approx 10^{10}$ cm^3, resulting in $s \approx 0.1$ cm. Thus, molecular ions are likely to undergo multiple charge exchange collisions within the sheath, thereby decreasing their incident energies at the surface and atomic ions will not undergo any collisions and arrive at the surface with the entire sheath drop potential. See Ref. 9 for additional discussion and the corresponding ion energy distributions.

Nitriding of the 6Al4V titanium alloy (6% aluminum, 4% vanadium) was carried out in both pulsed and continuous e-beam generated plasma systems. Titanium has a critical phase transition at 700 °C, which renders the strong, lightweight material very brittle. When subjected to the pulsed e-beam system as in Ref. 10 (90% N_2/10% Ar at 120 mT, -300 V_{dc} bias, $T_{surface} \approx 530$ °C, 1 ms pulse width and 50% duty factor) the nitriding process was very slow and incorporated a significant amount of oxygen in the titanium surface (39% Ti, 41% N, 20% O at. % at ~16 nm depth). Using a recently developed continuous e-beam system (90% N_2/10% Ar at 65 mTorr, and a -150 V_{dc} bias), the nitriding results improved significantly. Figure 8 shows the x-ray diffraction measurements at various surface temperatures. Since x rays do not penetrate titanium significantly, these spectra were less dramatic than in the previous stainless steel experiments. The critical information from these spectra is the evolution of the relatively small peaks located by dotted lines, which are attributed to TiN formation.[23] (The remaining peaks were due to the bulk Ti substrate.) All of these samples acquired a gold cast to their surface, a visual indication of the presence of TiN and there was also no noticeable phase transition of the titanium, which would have disrupted the consistent substrate peaks in the spectra. Furthermore, the implementation of the continuous e-beam source likely reduced the formation of surface oxides in the process as observed in the pulsed plasma experiments. By eliminating the plasma

Downloaded 26 Apr 2007 to 132.250.158.37. Redistribution subject to AIP license or copyright, see http://pop.aip.org/pop/copyright.jsp

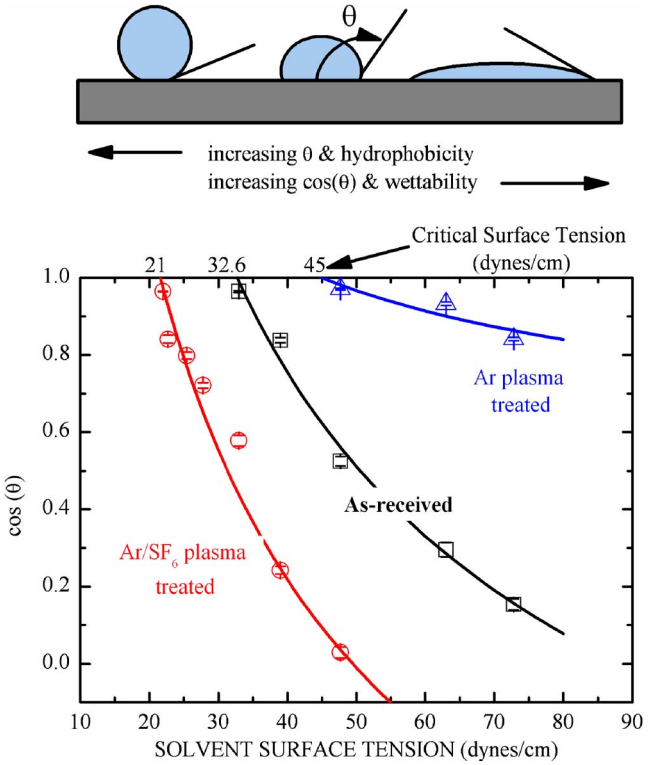

FIG. 9. (Color online) Critical surface tension extrapolation (from Ref. 24) of polyethylene treated with argon plasma and argon/SF_6 plasma.

off time, vacuum contaminants (H_2O, O_2) were less likely to form oxides on the surface and inhibit the formation of the nitride. In addition, the lower operating pressure used with the continuous plasma source resulted in a longer mean free path for the plasma ions and therefore a less collisional sheath, which could further assist in the surface diffusion process. Additional surface analyses and higher temperature experiments (up to the phase transition) are presently underway in our laboratory.

The final application topic to be discussed takes advantage of the low ion energy attribute of e-beam generated plasmas to modify the surface energy of polymeric materials. Pulsed plasmas containing 60 mTorr of pure Ar or Ar/SF_6 mixtures with 20%–30% SF_6 were exposed to polyethylene for 10 min and the surface free energy was determined *ex situ*. Changes in the surface energy were determined by the Zisman[24] approach, where the contact angles of solvents with a wide range of surface tensions were used to determine a critical surface tension associated with the surface. The critical surface tension is related to, but not necessarily, the actual surface energy. Contact angles were measured with respect to the droplet's interior solvent/substrate interface (see Fig. 9, top). Then cosines of the contact angles were then plotted with respect to the various solvent surface tensions and extrapolated to a completely wetted surface [$\theta = 0°$, $\cos(\theta) = 1$] to determine the critical surface tension. For polyethylene, the pure argon plasma can only change the surface physically (i.e., roughening), which increased the critical surface tension to 45 dyn/cm; with SF_6, the plasma chemically altered the surface and the critical surface tension decreased to 21 dyn/cm. These large changes in the polyethylene surface illustrate the wide range of control over both the chemical and physical processes available from plasma modification. The very low ion energies associated with the e-beam generated plasma reduce the minimum incident ion energies to below most chemical bond strengths without sacrificing reactive specie flux. Since the ion energy can also be increased by external biasing, the physical vs chemical mechanisms can be tailored to meet a specific final state of the surface.

V. SUMMARY AND CONCLUSION

In this work, the properties and basic phenomena associated with e-beam generated plasmas was presented. With a collinear magnetic field to reduce the effects of elastic scattering, sheets of multikilovolt electrons can be scaled to produce uniform, high density plasmas with low electron temperatures over active areas exceeding square meters. Since there are no external electric fields used to heat the plasma electrons, the plasma electron temperature is very low due to inelastic scattering off of gas molecules, independent of the plasma density. Thus, the plasma generation offers significant flexibility along a wide range of operating conditions. *In situ* diagnostics were used to illustrate basic plasma parameters and highlight the variation between the atomic and molecular ion dynamics. As in all plasmas, the diffusion of ions plays a critical role and can coexist with a more dominant recombination mechanism when molecular ion species are present.

Due to the unique features of e-beam generated plasmas, numerous phenomena in plasma physics and materials modification can be studied. The formation of a continuous ion-ion plasma was possible because the low electron temperature promotes attachment to the halogen-based gases and the fact that only the plasma electrons were confined by the collinear magnetic field. Developments of additional applications to surface nitriding and polymer modification were also presented. Both systems offer significant advances over conventional plasma systems, both in terms of the final product and the ability to interrogate the basic phenomena associated with the surface modification.

ACKNOWLEDGMENTS

The authors greatly appreciate the assistance of Dr. Chris Muratore (WPAFB, Materials Division) with the nitriding work and the Office of Naval Research for supporting this research.

[1] Z. Yu, J. J. Rocca, G. J. Collins, and C. Y. She, Phys. Lett. **96A**, 125 (1983).
[2] R. F. Fernsler, W. M. Manheimer, R. A. Meger, J. Mathew, D. P. Murphy, R. E. Pechacek, and J. A. Gregor, Phys. Plasmas **5**, 2137 (1998).
[3] W. M. Manheimer, R. F. Fernsler, M. Lampe, and R. A. Meger, Plasma Sources Sci. Technol. **9**, 370 (2000).
[4] S. G. Walton, D. Leonhardt, D. D. Blackwell, D. P. Murphy, R. F. Fernsler, and R. A. Meger, J. Vac. Sci. Technol. A **19**, 1325 (2001); D. Leonhardt, S. G. Walton, D. D. Blackwell, W. E. Amatucci, D. P. Murphy, R. F. Fernsler, and R. A. Meger, *ibid.* **19**, 1367 (2001).
[5] R. A. Meger, D. D. Blackwell, R. F. Fernsler, M. Lampe, D. Leonhardt, W. M. Manheimer, D. P. Murphy, and S. G. Walton, Phys. Plasmas **8**, 2558 (2001).
[6] S. G. Walton, D. Leonhardt, D. D. Blackwell, D. P. Murphy, R. F.

Downloaded 26 Apr 2007 to 132.250.158.37. Redistribution subject to AIP license or copyright, see http://pop.aip.org/pop/copyright.jsp

Fernsler, and R. A. Meger, Phys. Rev. E **65**, 046412 (2002).
[7]D. Leonhardt, S. G. Walton, C. Muratore, R. F. Fernsler, and R. A. Meger, J. Vac. Sci. Technol. A **22**, 2276 (2004).
[8]B. J. Orf, S. G. Walton, D. Leonhardt, G. S. Oehrlein, "Study of photoresist etching and roughness formation in electron-beam generated plasmas," J. Vac. Sci. Technol. B (in press).
[9]C. Muratore, S. G. Walton, D. Leonhardt, R. F. Fernsler, D. D. Blackwell, and R. A. Meger, J. Vac. Sci. Technol. A **22**, 1530 (2004).
[10]C. Muratore, D. Leonhardt, S. G. Walton, D. D. Blackwell, R. F. Fernsler, and R. A. Meger, Surf. Coat. Technol. **191**, 255 (2005).
[11]C. Muratore, S. G. Walton, D. Leonhardt, and R. F. Fernsler, J. Vac. Sci. Technol. A **24**, 25 (2006).
[12]D. Leonhardt and S. G. Walton, "The control and influence of ion energy in the deposition of SiO_2-like films," J. Vac. Sci. Technol. A (submitted).
[13]D. Leonhardt, S. G. Walton, C. Muratore, and R. A. Meger, Surf. Coat. Technol. **188-189**, 299 (2004).
[14]D. Leonhardt, C. Muratore, and S. G. Walton, IEEE Trans. Plasma Sci. **33**, 783 (2005).
[15]B. Chapman, in *Glow Discharge Processes: Sputtering and Plasma Etching* (Wiley, New York, 1980), p. 124.
[16]D. Leonhardt, C. Muratore, S. G. Walton, D. D. Blackwell, R. F. Fernsler, and R. A. Meger, Surf. Coat. Technol. **177-178**, 682 (2004).
[17]S. G. Walton, D. Leonhardt, and C. Muratore, IEEE Trans. Plasma Sci. **33**, 838 (2005).
[18]S. G. Walton, D. Leonhardt, R. F. Fernsler, and R. A. Meger, Appl. Phys. Lett. **81**, 987 (2002).
[19]V. Midha and D. Economou, J. Appl. Phys. **90**, 1102 (2001), and the references therein.
[20]S. G. Walton, C. Muratore, D. Leonhardt, R. F. Fernsler, D. D. Blackwell, and R. A. Meger, Surf. Coat. Technol. **186**, 40 (2004).
[21]A. V. Phelps, J. Phys. Chem. Ref. Data **20**, 557 (1991).
[22]M. A. Lieberman and A. J. Lichtenberg, *Principles of Plasma Discharges and Materials Processing* (Wiley, New York, 1994).
[23]JCPDS Powder Diffraction File, International Center for Powder Diffraction Data, Swarthmore, PA, 1998, Card 38-1420.
[24]A. H. Ellison and W. A. Zisman, J. Phys. Chem. **58**, 260 (1954).

Downloaded 26 Apr 2007 to 132.250.158.37. Redistribution subject to AIP license or copyright, see http://pop.aip.org/pop/copyright.jsp